crystals

MDPI

Article

Spectroscopic Characterization, Thermogravimetry and Biological Studies of Ru(III), Pt(IV), Au(III) Complexes with Sulfamethoxazole Drug Ligand

Eid H. Alosaimi

Department of Chemistry, College of Science, University of Bisha, P.O. Box 511, Bisha 61922, Saudi Arabia; ealosaimi@ub.edu.sa

Abstract: Complexes of Ru(III), Pt(IV), and Au(III) with sulfamethoxazole (SMX) were experimentally produced. The resulted formations of novel metal complexes were discussed using several techniques, such as effective magnetic moment molar conductivity, IR, UV, and 1H NMR spectra, elemental analyses, thermal analysis, microscopic and XRD analyses. The X-ray diffraction patterns of the solid powders of the synthesized sulfamethoxazole complexes indicated their identical formulation. The surface uniformity of the complexes' samples was confirmed by SEM images. These complexes appear as spots, dark in appearance, with particle sizes of 100–200 nanometers in transmission electron microscopy (TEM) pictures. The sulfamethoxazole ligand was shown to be bidentate coordinated to the metallic ions with sulfonyle oxygen and amido nitrogen groups, according to IR spectral data. Both Ru(III) and Au(III) complexes have an electrolytic nature, but the Pt(IV) complex has non-electrolytic properties. TG and DTG experiments proved the assigned composition and provided information regarding the thermal stability of complexes in a dynamic air atmosphere, according to the thermal analysis. The effect of the novel prepared complexes was examined for antibacterial and antifungal activity in vitro against a variety of pathogens, and they exceeded the sulfamethoxazole ligand in antibacterial activity. It was observed that the Pt(IV) complex has the ultimate activity versus all the assessed organisms relative to all compounds.

Keywords: sulfamethoxazole; transition metals; nanoparticles; spectroscopy; SEM; TEM

Citation: Alosaimi, E.H. Spectroscopic Characterization, Thermogravimetry and Biological Studies of Ru(III), Pt(IV), Au(III) Complexes with Sulfamethoxazole Drug Ligand. *Crystals* **2022**, *12*, 340. https://doi.org/10.3390/cryst12030340

Academic Editors: Assem Barakat, Alexander S. Novikov and Changquan Calvin Sun

Received: 27 January 2022
Accepted: 26 February 2022
Published: 2 March 2022

1. Introduction

Sulfamethoxazole (SMX) (4-Amino-*N*-(5-methylisoxazol-3-yl)-benzenesulfonamide) is a sulfonamide bacteriostatic antibiotic most commonly used in a 5:1 synergistic combination with trimethoprim in co-trimoxazole, also known by commercial names, such as Bactrim, Septrin, or Septra; in Eastern Europe, it is known as Biseptol. Its primary priorities are sensitive types of *Streptococcus*, *Staphylococcus aureus*, *E. coli*, *Haemophilus influenzae*, and *oral anaerobes* [1–9].

Antibacterial drugs, known as sulfonamides, include sulfamethoxazole (SMX), sulfadimethoxine (SDMX), and sulfadiazine, as well as others. Heavy metal is required for all forms of life. Heavy metals' antimicrobial effect makes them more important in field medicine. The antimicrobial and antibacterial activities of sulfonamides in association with heavy metals have enhanced their importance in the field of sulfonamide metal complexes [3].

Antibiotic sulfamethoxazole (SMX) is used to treat bacterial infections, such as bronchitis, prostatitis, pneumonia, urinary tract infections, middle ear infections and others. It also inhibits Gram-positive and Gram-negative bacteria, such as *Escherichia coli* and *Staphylococcus aureus* [10]. Sulfonamides have recently played a major role as an active functional group of (SMZ) medications, as well as via the combination of other functional groups, allowing the generation of various pharmacological compounds with anti-diabetic, antibacterial, and anti-tumor properties. [11–14]. Sulfamethoxazole (SMX) molecules include donating atoms

(O, N, and S) at many locations, allowing them to function as multi-dentate ligands. As a result, they can chelate with a variety of metal ions and structural kinds [15]. It was also reported that coordination with metal ions improves the pharmacological activity of these compounds [16–19]. For example, the Ag(I)-sulphadiazine complex can be used to treat skin burns [20,21], while the Zn(II) complex can be used to prevent the infections caused by bacteria in dead animals from fires [22,23]. The biochemical interaction of copper complexes with non-steroidal anti-inflammatory medications (NSAIDs) has been taken into account. Numerous Cu(II) complexes of NSAIDs with better antiulcerogenic and anti-inflammatory activity have been shown to minimize gastrointestinal toxicity [24]. Vanadium compounds have also been studied for their potential medicinal anti-diabetic effects [25,26]. From the literature, we did not find any biological features of nickel complexes [27–30]. Adamo et al. in [31] compared the activity of SMX and the complexes of (Co(II)) and Cu(II) against *S. aureus* and *E. coli*; they found that the hazard of the activity was improved. The improved performance of the complexes is due to chelation, with the increase in lipophilic properties ultimately decreasing the polarity of the metal atom, allowing it to permeate through the bacterial membrane's lipid layers [32,33]. As a result, [Co($C_{10}H_{11}N_3O_3S$)] and [Cu($C_{10}H_{11}N_3O_3S$)] could be used as lead compounds for developing antibiotics against the bacteria strains studied (*S. aureus* and *E. coli*) [31].

The biological features of sulfamethoxazole complexes with Au(III), Cd(II), Ni(II), and Zn(II) have been investigated in many papers [29–40]. It is worth noting that sulfamethoxazole Au(I) and Ag(I) compounds were earlier synthesized and described using X-ray diffraction, with the influence of these complexes on Gram-negative and Gram-positive microorganisms being examined [30]. The composition and characteristics of synthesized silver nanoparticles (AgNPs) and the MTT assay recorded the low cytotoxicity of the studied AgNPs; these nanoparticles are incredibly valuable as anti-biofilm and disinfectant components [34,35].

The current study is organized as follows: In Section 2, the synthesis and antimicrobial assay of the proposed complexes are presented. The results and discussion, including structural interpretations, thermal analysis and antibacterial activity of all the complexes, is investigated in Section 3. Section 3 concludes the findings of the paper.

These results encouraged us to create novel therapeutic transition metal complexes, with Au (III), Pt(IV), Ru(III), and complexes being particularly relevant medically to study the combined antimicrobial activity effect of drug chelation in conjunction with the metal ions.

2. Experimental Methods

2.1. Chemicals and Equipment

In this work, the purity of the used chemicals was very high and did not require any additional purification. Sigma-Aldrich Chemical Company, (St. Louis, MO, USA) provided sulfamethoxazole, $CaCl_2$, $ZnCl_2$, $RuCl_3$, $PtCl_4$, and $AuCl_3$. The prepared complexes were structured and analyzed by the following equipment (Table 1).

2.2. Method of Synthesis

Three sulfamethoxazole compounds were prepared through combining 1.0 mM $RuCl_3$, $PtCl_4$, $AuCl_3$ in 30 mL methanol with 1.0 mM sulfamethoxazole medicine in 30 milliliters of methanol. The reactant blends were refluxed for approximately three hours on a hotplate to produce the stained precipitates. The resultant complexes were purified, rinsed in hot methanol, dehydrated, and placed in a desiccator after cooling. Around 75–79% was the yield of the product. The component achieved has a greater melting point > 237 °C. Table 1 summarizes the physical data of the prepared complexes.

Table 1. Equipment used for measurements of data analyzed.

Type of Analysis	Models
Analyses of the elements	Perkin Elmer CHN 2400
Conductance	Jenway 4010 conductivity meter
FTIR spectra	Bruker FTIR Spectrophotometer
Raman laser	Bruker FT Raman with laser 50 mW
^{1}H NMR spectra	Varian Mercury VX-300 NMR spectrometer, 300 MHz
Electronic spectra	UV2 Unicam UV/Vis Spectrophotometer
Magnetic moment	Balance of Magnetic Susceptibility
SEM	Quanta FEG 250 equipment
XRD	X 'Pert PRO PANanalytical, with copper target
TEM	JEOL 100 s microscopy

2.3. Antimicrobial Assay

The antimicrobial action of the SMX and its metal ligands against bacteria (*B. subtilis*, *S. aureus*, *E. coli*, and *P. aeruginosa*) was investigated, utilizing the disc diffusion method [9]. Each mixture was solubilized in dimethylsulfoxide (DMSO) to form a solution of 110^{-3} M. The diffusion discs were infused with 10 microliters of the complex amount and put on the immunized coagulated form (Muller Hinton Agar). The dishes were kept at room temperature for 1 h before being incubated at 37 °C for 24 h. At the end of an incubation cycle, the inhibition zones (mm) were measured. Samples with DMSO were used as a control.

2.4. Estimation of Cytotoxic Impacts of Particular Chemical Complex

Mammalian cell lines: MCF-7 cells (cancer cell line of human breast) and HepG-2 cells (human hepatocellular carcinoma) were attained from the VACSERA Tissue Culture Section.

Materials: Dimethyl sulfoxide (DMSO), trypan blue dye and crystal violet were obtained from Sigma Aldrich (St. Louis, MO, USA).

DMEM, RPMI-1640, fetal bovine serum, L-glutamine, HEPES buffer solution, gentamycin and 0.25% Trypsin-EDTA were purchased from Lonza, Switzerland.

Stain of crystal violet (1%): The stain comprised 0.5% (*w*/*v*) crystal violet and 50% methanol, later filled to the mark to volume with dist.H_2O and purified with a filter paper of Whatman No.1.

Cell line Propagation: The cells were reproduced 0in Dulbecco's altered Eagle's medium (DMEM) accompanied in addition to 10% thermal-deactivated embryonic bovine serum, 1% L-glutamine, HEPES buffer and 50 µg/mL gentamycin. The whole cells were retained at 37 °C in a saturated atmosphere with 5% CO_2 and were sub-cultured twice in seven days.

Evaluation of cytotoxicity through practicality assay: In order to evaluate the cytotoxicity assay, the cells were planted in 96-well plate at a cell dilution of 1×10^4 cells per well in 100 microliters of growth medium. Freshly prepared growth media comprising distinct amounts of the analysis were incorporated in the manner of 24 h of seeding. Sequential two-fold concentrations of the analyzed biological components were included by merging cell monolayers distributed into 96-well, flat-bottomed microtiter plates (Falcon, Middlesex, NJ, USA) using a multichannel pipette. The microtiter plates were incubated at 37 °C in a humidified oven with 5% CO_2 for an interval of one complete day. Three wells were utilized for every single strength of the assessment trial. The standard cells' so-called control were incubated, not including the analyzed sample and without or with solvent DMSO. The small percentage of DMSO that appeared in the wells (maximal 0.1%) was found not to influence the trial. Later, incubation of the cells was performed at 37 °C for 24 h; the possible cells recovery was characterized by a spectrophotometer method. In summary, following the result of the incubation period, media were extracted, and the crystal violet solution (1%) was incorporated to individual wells for at least half an hour. The

stain was separated, and the plates were cleansed utilizing distilled water until the whole additional stain was separated. Glacial acetic acid (30%) was subsequently incorporated to all wells and blended comprehensively, and then again, the absorbance of the samples was determined after being softly stirred on a Microplate reader (TECAN, Inc., Männedorf, Switzerland), utilizing a wavelength of 490 nm. The complete outcomes were corrected for background absorbance identified in wells, not including the stain. The samples after treatment were evaluated with the cell control in the non-existence of the tested compounds. All experiments were carried out in triplicate. The cell cytotoxic influence of the individually analyzed complex was assessed. The optical density was determined by the microplate reader (SunRise, TECAN, Inc., Morrisville, NC, USA) to calculate the number of viable cells, and the proportion of possibility was considered as [(ODt/ODc)] × 100%, where ODt is the mean optical density of wells activated with the sample of interest and ODc is the mean optical density of cells not treated, on the other hand. The correlation among the remaining cells and dose of the drug strength is mapped to obtain the persistence curve of each tumor cell line after treatment with the particular mixture, the 50% inhibition strength (IC_{50}), the amount desired to cause toxic properties in 50% of integral cells, was assessed from graphic plots of the dosage response curve for each conc., using Graph pad Prism software (San Diego, CA, USA) [7,8].

3. Results and Discussion

3.1. Conductance and Microanalytical Studies

The latest Au(III), Pt(IV), Ru(III) and metal complexes with SMX were stable, colorful, and non-hygroscopic in nature. In dimethyl sulfoxide and dimethyl formamide, the complexes were soluble. The superb tangible characteristics and distinct information of the synthesized ligand and its existing metal complexes were quantified. Au(III), Pt(IV), Ru(III) and complexes have the usual formulas $[Ru(smx)(H_2O)_2Cl_2]Cl$ (1), $[Pt(smx)(H_2O)Cl_3]$ (2), and $[Au(smx)Cl_2]Cl{\cdot}H_2O$ (3), correspondingly, according to elemental studies (Table 1). The molar conductance of SMX in the free state is 0.170 Ω^{-1} mol^{-1} cm^2 at room temperature, whereas the identical data point for metal complexes is described to range from 0.200 and 47.60 Ω^{-1} mol^{-1} cm^2. In contrast to SMX, conductance data showed that the Ru(III) and Au(III) complexes were electrolytes, but Pt(IV) was a non-electrolyte [38]. The complexes' elemental analyses results (Table 2) are compared with the complexes' postulated structures, as indicated in Scheme 1.

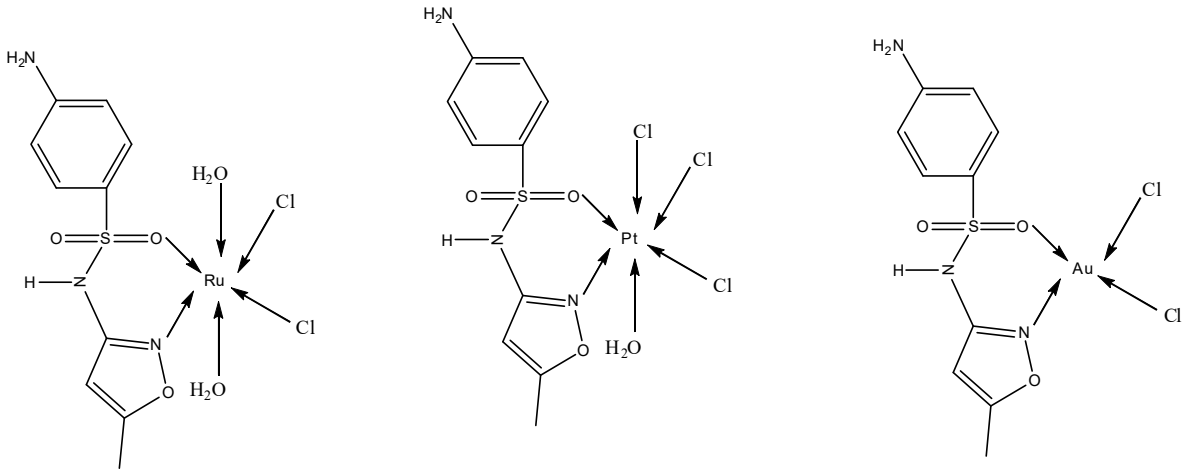

Scheme 1. SMX coordination mode with Ru(III), Pt(IV), and Au(III).

Table 2. Physico-analytical and elemental analysis data for sulfamethoxazole and its metal complexes.

Complex (MF) Mwt.	Yield%	mp/°C	Color	Magnetic Moment (BM)	Conductance ($ohm^{-1} \cdot cm^2 \cdot mol^{-1}$)	Element	Calc.	Found
($C_{10}H_{11}N_3O_3S$) (smx) (253)	-	140	White	Diamagnetic	0	%C	47.43	46.21
						%H	4.34	3.22
						%N	16.60	15.36
						%M	-	-
						%S	-	-
						%Cl	-	-
$[Ru(C_{10}H_{11}N_3O_3S)(H_2O)_2Cl_2]Cl$ (496.74)	85	337	Dark green	1.65	46.80	%C	24.18	24.34
						%H	3.04	3.11
						%N	8.46	8.79
						%M	20.35	20.14
						%S	6.46	6.22
						%Cl	21.41	21.01
$[Pt(C_{10}H_{11}N_3O_3S)(H_2O)Cl_3]$ 572.73	90	258	Brown	Diamagnetic	0.200	%C	20.97	20.23
						%H	2.29	2.32
						%N	7.34	7.25
						%M	34.06	34.03
						%S	5.60	5.58
						%Cl	18.57	18.00
$[Au(C_{10}H_{11}N_3O_3S)Cl_2]Cl \cdot H_2O$ 574.62	88	216	Pale yellow	Diamagnetic	47.60	%C	20.90	20.54
						%H	2.28	2.25
						%N	7.31	7.46
						%M	34.28	34.45
						%S	5.58	5.45
						%Cl	18.51	18.51

3.2. FT-IR Spectral Studies

As KBr discs, the IR bands of Au (III), Pt(IV), Ru(III) and complexes, as well as free sulfamethoxazole, were examined (Figure 1). The complexes' infrared spectra are compared to that of free SMX to establish the position of coordination that may be implicated in chelation. The functional groups contributing to the coordination are allocated stretching vibration bands (Table 3). The free ligand shows two strong bands at 3466 cm^{-1}, 3377 cm^{-1} and 3298 cm^{-1}, relating to the asymmetric and symmetric stretching vibrations of the aromatic amino group (NH_2) and sulfonamide (NH), respectively [39]. After chelation, the C=N stretching vibration peak in SMX shifted to elevated frequency values at 1693 cm^{-1} designed for Ru(III) and to lower frequency values at 1606 cm^{-1} and 1608 cm^{-1} used for Pt(IV) and Au(III) complexes, correspondingly [3]. Here, the S=O group's asymmetric and symmetric stretching vibrations of SMX were found at 1365 cm^{-1} and 1091 cm^{-1}, respectively [40]. The shift of the asymmetric stretching vibration of S=O to lower values at 1330 cm^{-1}, 1330 cm^{-1} and 1314 cm^{-1} in the Ru(III), Pt(IV), and Au(III) complexes, correspondingly, indicates that SMX is linked to the metal ion by a single oxygen atom in the sulfonyl group (S=O). Stretching of the phenyl ring (C=C) gives infrared bands at 1596 cm^{-1} and 1503 cm^{-1}. The phenyl ring vibrations were noted to be comparatively unshifted in the spectra of metal complexes, and isoxazole ring vibrations were observed in the free sulfa molecule spectrum at 1471 cm^{-1} and 1438 cm^{-1}. For metal complexes, the comparatively unshifted band at 1471 cm^{-1} and 1438 cm^{-1} with regard to isoxazole ring vibrations revealed a slight or weak interface among the isoxazole nitrogen and metal ion. New bands in regions of 545–578 cm^{-1} and 412–499 cm^{-1} in the complex's spectra are designated to M–O and M–N stretching vibrations, correspondingly. The non-existence of these bands as of the spectrum of SMX validates the bonding of the metal ion over the NO linkage of C=N and S=O groups.

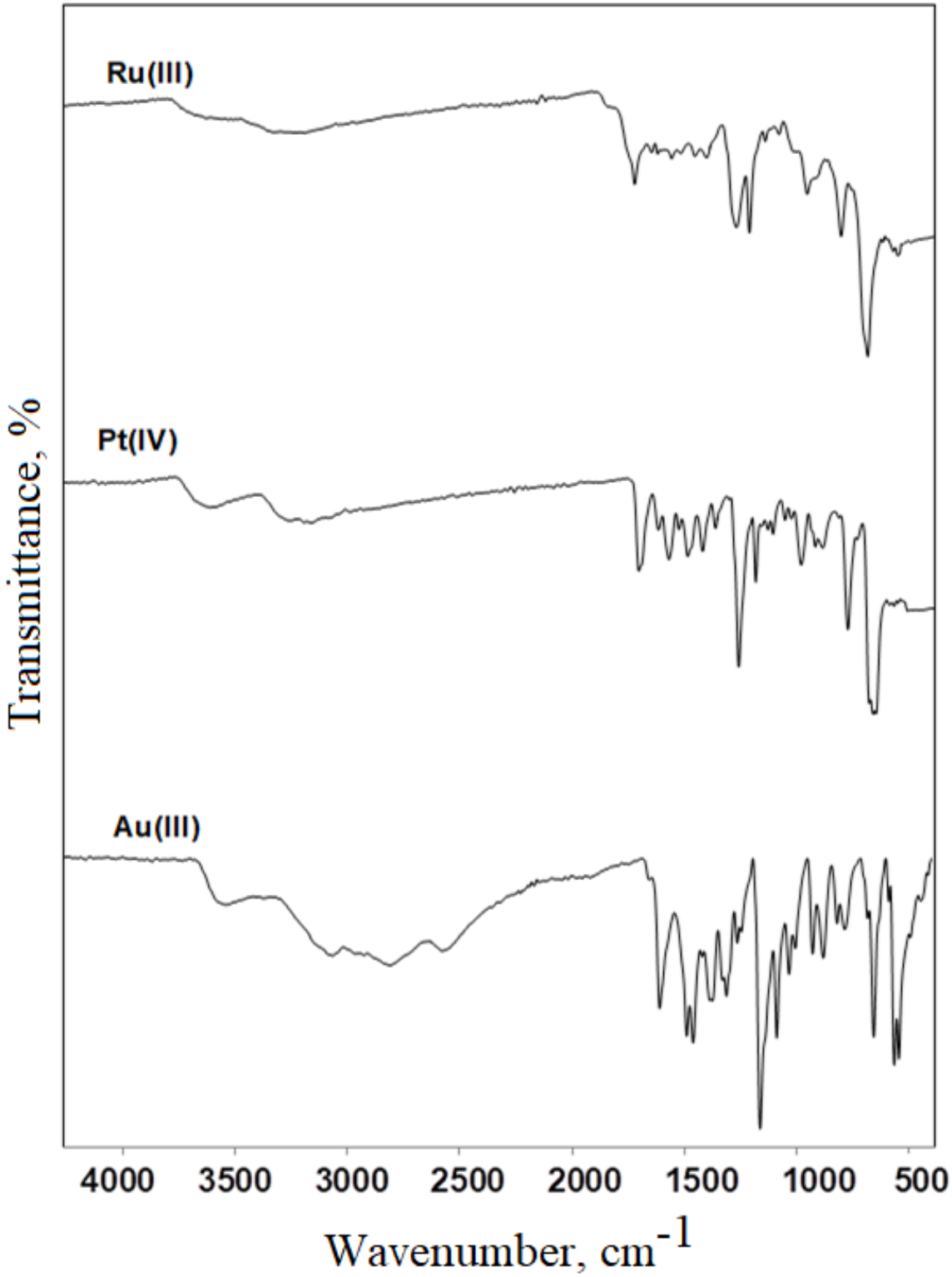

Figure 1. Infrared spectra for SMX and their metal complexes.

Table 3. IR frequencies (cm^{-1}) and provisional positions for sulfamethoxazole, Au-sulfamethoxazole, Pt-sulfamethoxazole, and Ru-sulfamethoxazole complexes.

IR Frequencies				Assignments
SMX	Au(III)	Pt(IV)	Ru(III)	
3466	3549	3508	3495	$\nu_{as}(NH_2)$, aniline
3377	3357	-	-	$\nu_{s}(NH_2)$, aniline
3298	-	3156	3211	ν(-NH), sulfonamide
3143	-	3094	3193	ν(C-H), isoxazole ring
2989	2956	2968	-	$\nu(CH_3)$
1621	1608	1606	1693	ν(C=O) isoxazole ring
1596	1487	1520	1594	ν(C=N)
1503	1462	1470	1495	isoxazole ring vibrations
1383	1386	1392	1390	$\nu_{as}(SO_2)$; asymmetric
1266	1262	1266	1277	ν_{s}(C-N) sulfonamide
1091	1089	1089	1083	$\nu_{s}(SO_2)$; symmetric
927	929	933	914	ν(S-N)
884	883	887	894	ν(C-H) isoxazole ring
831	821	828	828	δ(C-H)
684	657	677	677	ν(C-S)
575	566	578	562	ν(M-O)
426	414	412	420	ν(M-N)

3.3. Electronic Spectra

UV-visible spectra confirmed the development of the metal sulfamethoxazole complexes. Table 4 reveals the microelectronic absorption spectra of SMX, as well as the Au (III), Pt(IV) and Ru(III) complexes, in the wavelength ranging from 200 to 800 nm. Free SMX is reproduced at 298,322 nm and 366 nm, which can be accredited to n-π* and π-π* transitions. These shifts occur when unsaturated hydrocarbons with ketone groups are present [41]. The disappearance of the band at 298 nm in complexes; the shift of the reflection bands to elevated numbers (bathochromic shift); and the occurrence of new bands in the absorption spectra of complexes revealed the development of their metal complexes [30]. Bands in the region of 396 nm to 418 nm were also seen in the complexes, which are attributed to the ligand-to-metal charge transfer [41,42].

Table 4. UV-Vis. spectrum of sulfamethoxazole, Au(III), Pt(IV), Ru(III), and complexes.

Assignments (nm)	SMX	SMX Complex with		
		Ru(III)	Pt(IV)	Au(III)
n-π* transitions	366	378	376	386
π-π* transitions	298,322	338	338	336
d–d transitions	-	572	570	-
Ligand–metal charge transfer	-	396	418	400

3.4. ^1H NMR Spectra

NMR (nuclear magnetic resonance) spectroscopy confirmed the hypothesized molecular structures of the metal complexes. Figure 2 represents the ^{1}H NMR spectra of Au(III), and Pt(IV) complexes carried out in DMSO-d_6 as a solvent. The ^{1}H NMR spectra of sulfamethoxazole (Table 5) showed at δ: 2.25–2.50 ppm relating to -CH_3, at δ: 6.32 ppm according to -NH_2 group, at δ: 7.50 ppm for -CH aromatic and at δ: 10.99 ppm due to SO_2–NH group. When the main peaks of SMX are compared to their complexes, it is detected that all of the peaks of the free ligand appear in the spectra of the complexes with shifts as a result of complexation. New peaks are observed at δ: 3.95, which could be attributed to the presence of water molecules in the complexes [43–45].

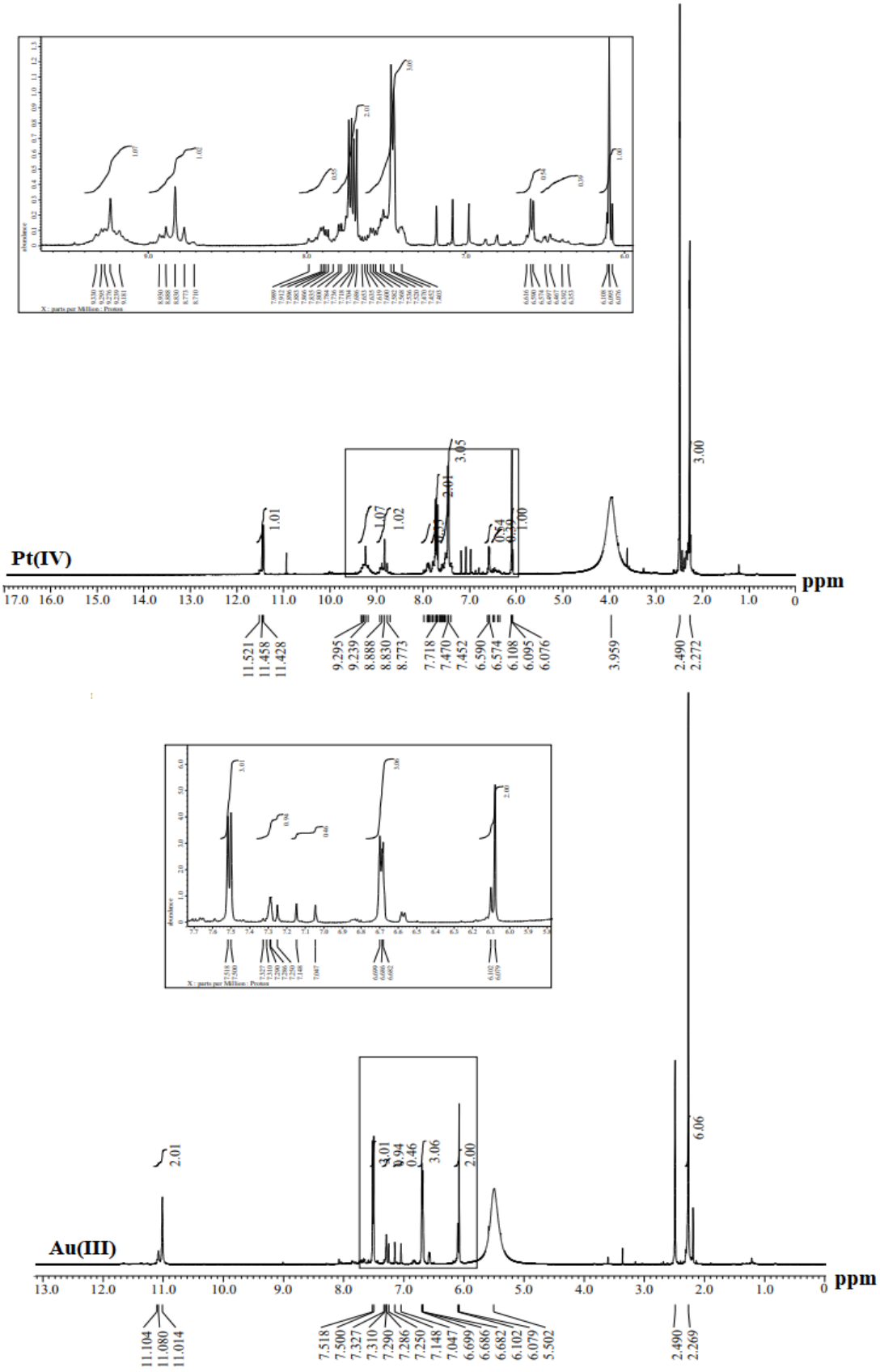

Figure 2. ^{1}H NMR spectrum for Au(III) and Pt(IV), complexes.

Table 5. ^{1}H NMR data (ppm) and tentative transitions for (A) sulfamethoxazole; (B) [Pt(smx)(H_2O)Cl_3] (2), and (C) [Au(smx)Cl_2]Cl·H_2O.

A	B	C	Assignments
2.25, 2.50	2.21, 2.49	2.26, 2.49	δ H, (s,3H,-CH_3)
-	3.95	3.95	δ H, (s,2H,H_2O)
6.32	6.56	6.62	δ H, (m,2H,NH_2)
7.50	7.41–7.74	7.90	δ H, (m,5H,Ar-CH)
10.99	11.50	11.10	δ H, (s,H,SO_2-NH)

3.5. Thermal Analysis

To confirm the structures of [Ru(smx)(H_2O)$_2Cl_2$]Cl (1), [Pt(smx)(H_2O)Cl_3] (2) and [Au(smx)Cl_2]Cl·H_2O (3) (Figure 3). TG analyses were carried out under nitrogen at 10 °C min^{-1}. Table 6 shows the results of the weight loss, lost species under the effect of the variations of temperature. According to the results, sulfamethoxazole breakdown began at 25 °C and ended at 795 °C. SMX decomposition peaks at 113, 266 and 378 °C, resulting in a loss of weight of about 77.7%, equivalent to the loss in weight of $3C_2H_2$ + CH_4 + HCN + NO_2 + NO and S + 2C in the final thermal decomposition product obtained. There are two degradation steps in the thermal decomposition of the [Ru(smx)(H_2O)$_2Cl_2$]Cl complex. When two coordinated water molecules are heated to a highest temperature of 169 °C in the first stage, the Ru(III) complex is lost, along with weight loss (7.25%). The second stage of deterioration takes place at extreme temperatures of 312 °C and 402 °C and is escorted by a loss in weight (73.22%) subsequent to the loss of $5C_2H_2$ + HCl + Cl_2 + $1.5N_2$ + SO; then, the decisive thermal decomposition product obtained is RuO_2. There are two degradation steps in the thermal decomposition of the [Pt(smx)(H_2O) Cl_3] complex. The Pt(III) complex loss upon heating one coordinated molecule of water in the initial step at highest temperature 175 °C is associated with a loss in weight of 3.14%. The next step of decomposition, which ensues at highest temperatures of 226 °C and 287 °C, is accompanied by weight loss (60.35%), which corresponds to the loss of $5C_2H_2$ + 3HCl + $1.5N_2$ + SO_2, then the concluding thermal decay product achieved is PtO_2. The thermal decomposition of [Au(smx)Cl_2]Cl·H_2O complex exhibits two degradation steps. At an extreme temperature of 100 °C, the first step of decomposition appears, which is attended by a loss of weight (3.13%), this relates to the loss of one water molecule. The second stage of decomposition takes place at temperatures between 242 and 476 degrees Celsius and is attended by a weight loss of 62.60%, which resembles the decrease in $5C_2H_2$ + 3HCl + N_2O + NO + SO_2; then, the ultimate thermal decomposition product obtained is Au.

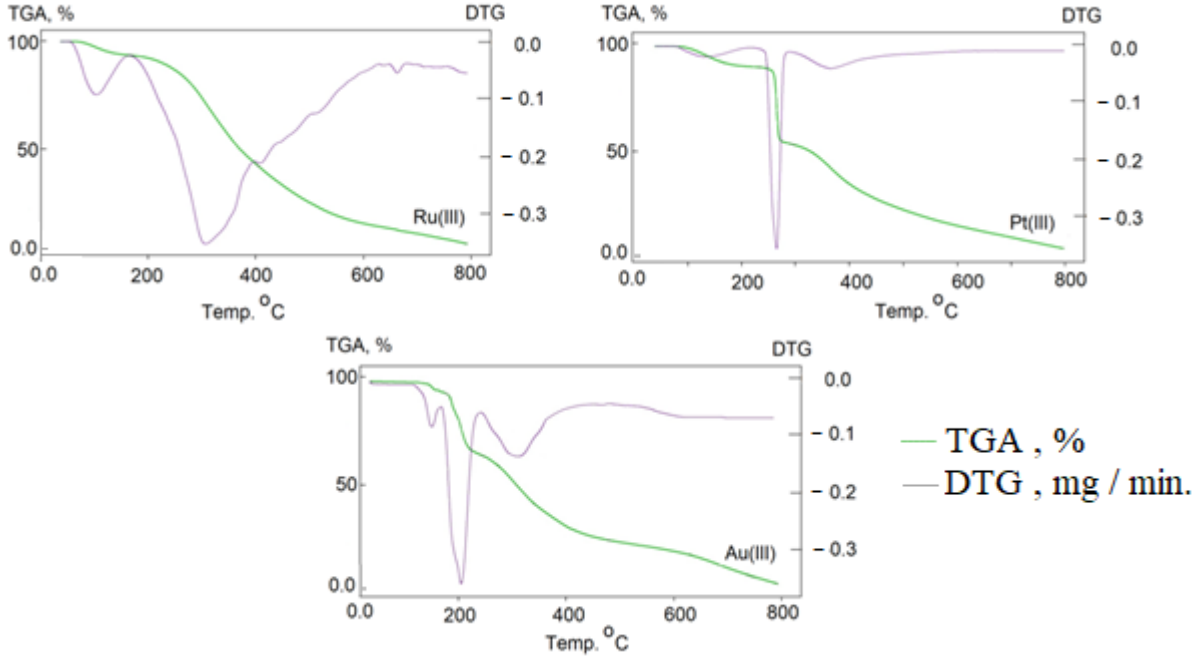

Figure 3. TGA and DTG diagram for Pt(IV), Au(III) and Ru(III) complexes.

Table 6. The extreme temperature T_{max} (°C) and weight deficiency data of the decomposition stages for sulfamethoxazole, Pt(IV), RU(III)and Au(III) complexes.

Compounds (M. F) M.wt	Decomposition	Weight Loss (%)		T_{max} (°C)	Lost Species
		Found	Calc.		
Sulfamethoxazole (smx)	First step	77.87	78.85	113, 266, 378	$3C_2H_2 + CH_4 + HCN + NO_2 + NO$
253 ($C_{10}H_{11}N_3O_3S$)	Total loss	77.77	78.85		S + 2C
	Residue	22.13	21.15		
[Ru($C_{10}H_{11}N_3O_3S$)(H_2O)$_2Cl_2$]Cl (1)	First step	7.15	7.25	169	$2H_2O$
496.74 ($RuC_{10}H_{15}Cl_3N_3O_5S$)	Second step	65.90	65.96	312, 402	$5C_2H_2 + HCl + Cl_2 + 1.5N_2 + SO$
	Total loss	73.05	73.22		RuO_2
	Residue	26.95	26.78		
[Pt($C_{10}H_{11}N_3O_3S$)(H_2O)Cl_3] (2)	First step	3.10	3.14	175	H_2O
572.73 ($PtC_{10}H_{13}Cl_3N_3O_4S$)	Second step	57.00	57.21	226, 287	$5C_2H_2 + 3HCl + 1.5N_2 + SO_2$
	Total loss	60.10	60.35		PtO_2
	Residue	39.90	39.65		
[Au($C_{10}H_{11}N_3O_3S$)Cl_2]Cl·H_2O (3)	First step	3.11	3.13	100	H_2O
574.62 ($AuC_{10}H_{13}Cl_3N_3O_4S$)	Second step	62.79	62.60	242, 476	$5C_2H_2 + 3HCl + N_2O + NO + SO_2$
	Total loss	65.90	65.73		Au
	Residue	34.10	34.27		

3.6. Morphological Studies

To study the surface morphology of our synthesized complexes, Au(III), Pt(IV), and (Ru(III), sulfamethoxazole), (XRD) X-ray powder diffraction, transmission electron microscopy (TEM) and scanning electron microscopy (SEM) were utilized. The morphology and particle size of the studied complexes were assessed using SEM. The SEM images of the samples are displayed in Figure 4; all complexes have a uniform shape. The Ru(III), Pt(IV), and Au(III) sulfamethoxazole complexes' TEM images indicate particle sizes of 100 nm, 200 nm, and 100 nm, respectively (Figure 5). The complexes' powder XRD patterns reveal strong crystalline peaks, indicating that they are in the crystalline phase. Scherr's equation [46] can be used to determine the crystallite size of these complexes (D) as patterns of XRD from full width at half maximum of the distinctive peak. These complexes have crystallite sizes of 100 nm, 200 nm, and 100 nm, according to XRD.

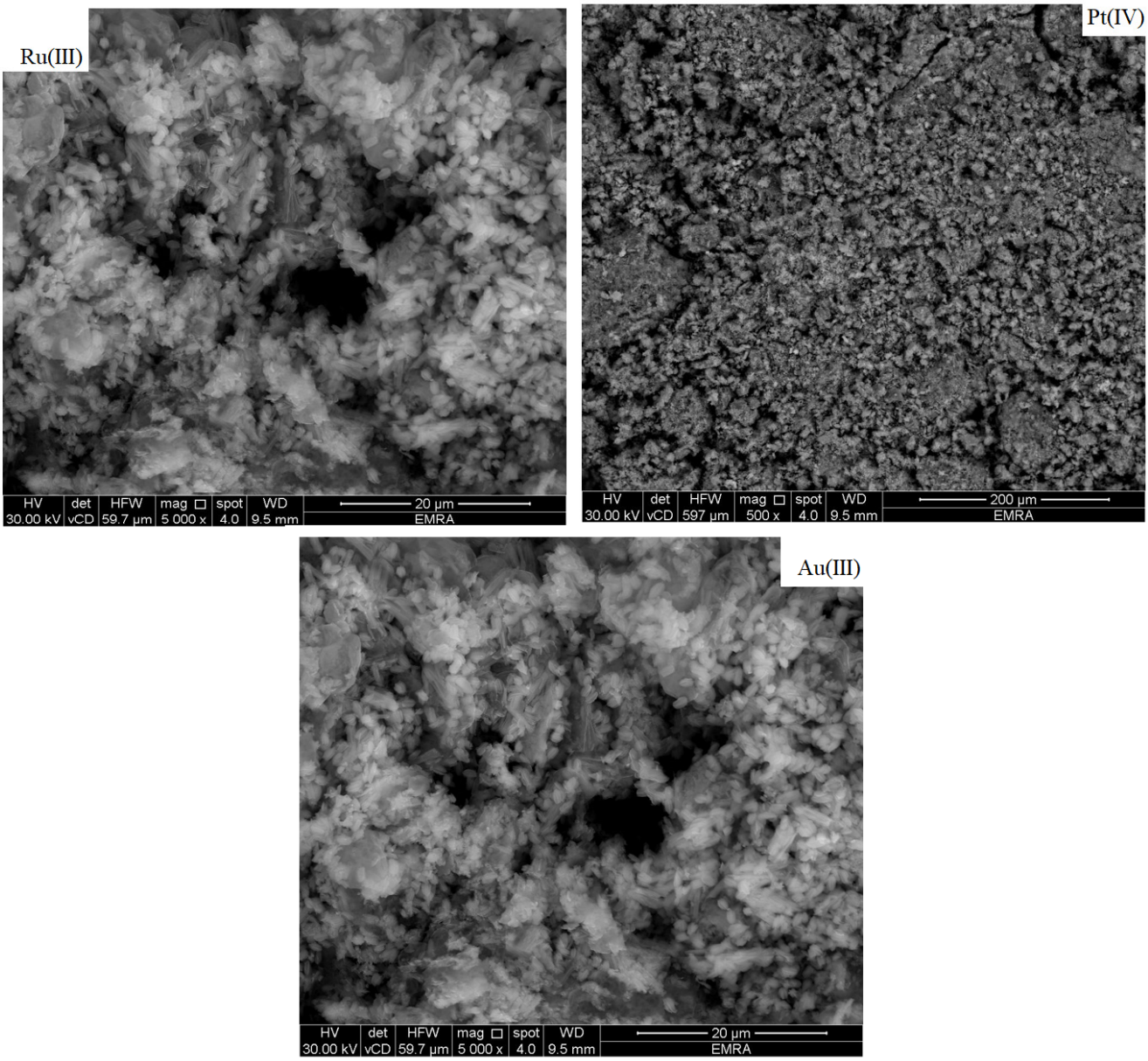

Figure 4. SEM images of for Au (III) Pt(IV), and Ru(III), complexes.

3.7. Biological Activity

To assess the biological capability of SMX and their metal complexes, they were investigated with different bacterial strains. The effect of the novel prepared complexes on the bacterial activity is reported in Table 7 and Figure 6. The results revealed that the newly synthesized complexes have noticeable bactericidal activity and their activities increased when complexed with the metal ions. The biological activity of our prepared complexes was tested in comparison with the SMX ligand. The sequence of inhibitory capacities growth was: Ampicillin > Pt(IV) > Au(III) > SMX > Ru(III) (for *B. subtilis*), Ampicillin > Pt(IV) > Au(III) > SMX > Ru(III) (for *S. aureus*), Ampicillin > Pt(IV) > Au(III) > SMX > Ru(III) (for *E. coli*), Ampicillin > Pt(IV) > Au(III) > Ru(III) > SMX (for *P. aeruginosa*). We concluded from these results that metal complexes have a remarkable activity against pathogenic bacteria and that explained on the basis of chelation theory the chelation could facilitate the ability of a complex to cross a cell membrane of the pathogens and also ease their diffusion through the lipid layer of spore membrane to the site of action and ultimately killing them [44,45,47].

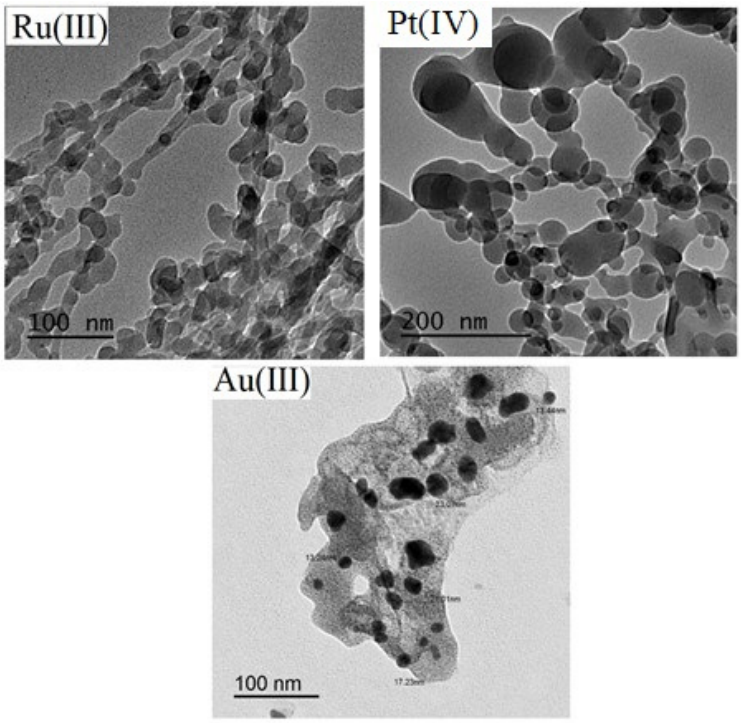

Figure 5. TEM images of Au (III) Pt (IV), and Ru(III), complexes.

Table 7. Results of antibacterial activity of the prepared complexes.

Compounds	Microbial Species			
	B. subtilis	***S. aureus***	***E. coli***	***P. aeruginosa***
SMX	10 ± 0.2	15 ± 0.11	9 ± 0.03	6 ± 0.22
Ru(III)-SMX	$9^{NS} \pm 0.11$	$11^{NS} \pm 0.01$	$9^{NS} \pm 0.02$	$10^{+1} \pm 0.33$
Pt(IV)-SMX	$19^{+2} \pm 0.5$	$19^{+1} \pm 0.11$	$17^{+2} \pm 0.6$	$17^{+3} \pm 0.22$
Au(III)-SMX	$12^{+1} \pm 0.1$	$15^{NS} \pm 0.2$	$13^{+1} \pm 0.1$	$13^{+2} \pm 0.02$
Control (DMSO)	0	0	0	0
Ampicillin	26 ± 0.3	21 ± 0.02	25 ± 0.11	26 ± 0.05

Statistical significance P^{NS}; P not significant, $p < 0.05$; P^{+1}; P significant, $p > 0.05$; P^{+2}; P highly significant, $p > 0.01$; P^{+3}; P very highly significant, $p > 0.001$; student's *t*-test (Paired).

Anticancer activities of the synthesized sulfamethoxazole complexes are given in Table 8. Anticancer activity of the complexes follows the order: Au(III)-SMX > Au(III)-SMX > Ru(III)-SMX. The Au(III)-SMX complex showed higher inhibition activity than that of other Pt(IV)-SMX and Ru(III)-SMX complexes.

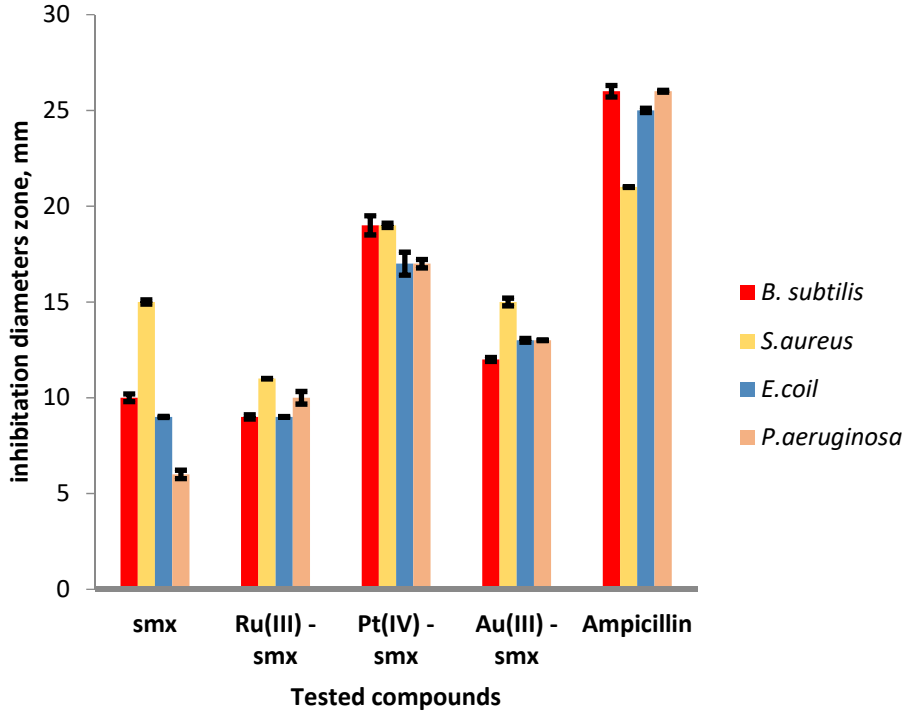

Figure 6. Statistical interpretation for biological action of sulfamethoxazole and its metal complexes.

Table 8. Results of Anticancer activity of the prepared complexes.

Sample Code	IC_{50} Values (µg/mL)	
	HepG-2	**MCF-7**
Au(III)-SMX	30 ± 2.1	41 ± 2.6
Ru(III)-SMX	110 ± 8.2	124 ± 9.7
Pt(IV)-SMX	70.9 ± 5.7	81 ± 6.1

4. Conclusions

SMX reactions with Ru(III), Pt(IV), and Au(III) ions resulted in the formation of new mononuclear complexes. Various analytical and spectral techniques were used to characterize the metal complexes and clarify their structures. The data revealed that SMX acted as a bidentate ligand. The latest results encourage the proposed octahedral architecture of metal complexes and result in a beneficial arrangement of molecules. The metal complexes surpassed the ligands in terms of bactericidal activity against various strains of bacteria, including *P. aeruginosa*, *E. coli*, *S. aureus*, and *B. subtilis.* The preliminary in vitro antibacterial screening activity revealed that the Pt(IV) complex showed moderate activity against tested bacterial strains and higher activity compared to the ligand, SMX. According to the molar conductivity data, the Ru(III) and Au(III) complexes are electrolytes, whereas Pt(IV) is not. The stoichiometry of 1:1 (M:L) is supported by the analytical data. The surface morphology and grain size of SMX complexes are between 100 and 200 nanometers in size.

Funding: This research received no specific grant from any funding agency in the public, commercial, or not-for-profit sectors.

Informed Consent Statement: Author consents to publication.

Data Availability Statement: On reasonable request, author will provide the datasets used and/or analyzed during the current work.

Acknowledgments: The author expresses his gratitude to the University of Bisha.

Conflicts of Interest: The author declares no conflict of interest.

Sample Availability: On reasonable request, author will provide the datasets used and/or analyzed during the current work.

References

1. Alias, M.F.; Abdul-Hassan, M.A. Synthesis and Characterization of Some Metal Complexes with their Sulfamethoxazole and 4,4′ -dimethyl-2,2′ -bipyridyl and study Cytotoxic Effect on Hep-2 Cell Line. *Baghdad Sci. J.* **2015**, *12*, 740–752.
2. Zahid, H.; Chohan Hazoor, A.; Shad, N.F.H. Synthesis, Characterization and Biological Properties of Sulfonamide Derived Compounds and Their Transition Metal Complexes. *Appl. Organ Metal. Chem.* **2009**, *23*, 319–328.
3. Chamundeeswari, S.V.; Samuel, E.J.J.; Sundaraganesan, N. Molecular structure, vibrational spectra, NMR and UV spectral analysis of sulfamethoxazole. *Spectrochim. Acta Part A Mol. Biomol. Spectrosc.* **2014**, *118*, 1–10. [CrossRef]
4. Hammoudeh, D.I.; Zhao, Y.; White, S.W.; Lee, R.E. Replacing sulfa drugs with novel DHPS inhibitors. *Future Med. Chem.* **2013**, *5*, 1331–1340. [CrossRef] [PubMed]
5. Scozzafava, A.; Owa, T.; Mastrolorenzo, A.; Supuran, C.T. Anticancer and Antiviral Sulfonamides. *Curr. Med. Chem.* **2003**, *10*, 925–953. [CrossRef] [PubMed]
6. Carta, F.; Supuran, C.T.; Scozzafava, A. Sulfonamides and their isosters as carbonic anhydrase inhibitors. *Future Med. Chem.* **2014**, *6*, 1149–1165. [CrossRef] [PubMed]
7. Mosmann, T. Rapid colorimetric assay for cellular growth and survival: Application to proliferation and cytotoxicity assays. *J. Immunol. Methods* **1983**, *65*, 55–63. [CrossRef]
8. Gomha, S.M.; Riyadh, S.M.; Mahmmoud, E.A.; Elaasser, M.M. Synthesis and Anticancer Activities of Thiazoles, 1,3-Thiazines, and Thiazolidine Using Chitosan-Grafted-Poly(vinylpyridine) as Basic Catalyst. *Heterocycles* **2015**, *91*, 1227–1243.
9. Nunes, J.H.B.; de Paiva, R.E.F.; Cuin, A.; Lustri, W.R.; Corbi, P.P. Silver complexes with sulfathiazole and sulfamethoxazole: Synthesis, spectroscopic characterization, crystal structure and antibacterial assays. *Polyhedron* **2015**, *85*, 437–444. [CrossRef]
10. *Sulfamethoxazole*; Drug Bank: Alberta, AB, Canada, 2015.
11. Toth, J.E.; Grindey, G.B.; Ehlhardt, W.J.; Ray, J.E.; Boder, G.B.; Bewley, J.R.; Klingerman, K.K.; Gates, S.B.; Rinzel, S.M.; Schultz, R.M.; et al. Sulfonimidamide analogs of oncolytic sulfonylureas. *J. Med. Chem.* **1997**, *40*, 1018. [CrossRef]
12. Medina, J.C.; Roche, D.; Shan, B.; Learned, R.M.; Frankmoelle, W.P.; Clark, D.L.; Rosen, T.; Jaen, J.C. Novel halogenated sulfonamides inhibit the growth of multidrug resistant MCF-7/ADR cancer cells. *Med. Chem. Lett.* **1999**, *9*, 1843. [CrossRef]
13. Yoshino, H.; Ueda, N.; Niijima, J.; Sugumi, H.; Kotake, Y.; Koyanagi, N.; Yoshimatsu, K.; Asada, M.; Watanabe, T. Novel sulfonamides as potential, systemically active antitumor agents. *J. Med. Chem.* **1992**, *35*, 2496. [CrossRef] [PubMed]
14. Owa, T.; Yoshino, H.; Okauchi, T.; Yoshimatsu, K.; Ozawa, Y.; Sugi, N.H.; Nagasu, T.; Koyanagi, N.; Kitoh, K. Discovery of novel antitumor sulfonamides targeting G1 phase of the cell cycle. *J. Med. Chem.* **1999**, *42*, 3789. [CrossRef] [PubMed]
15. Alias, M.F.; Hassan, M.M.A.; Khammas, S.J. Synthesis, characterization of some metal complexes with mixed ligands derived from sulfamethoxazole and 4, 4-dimethyl-2, 2-bipyridyl. *Int. J. Sci. Res.* **2015**, *4*, 2337–2342.
16. Karthikeyan, G.; Mohanraj, K.; Elango, K.P.; Girishkumar, K. Synthesis and spectral characterization of lanthanide complexes with sulfamethoxazole and their antibacterial activity. *Russ. J. Coord. Chem.* **2006**, *32*, 380–385. [CrossRef]
17. Mahind, L.H.; Waghmode, S.A.; Nawale, A.; Mane, V.B.; Dagade, S.P. Structural characterization of nanosized Fe_2O_3-CeO_2 catalysts by XRD, EDX and TEM techniques. *J. Pharm. Biosci.* **2013**, *5*, 2–105.
18. Mahmoud, W.H.; Mohamed, G.G.; Ele-Dessouky, M.I. Synthesis, Characterization and in vitro Biological Activity of Mixed Transition Metal Complexes of Lornoxicam with 1,10- phenanthroline. *Int. J. Electrochem. Sci.* **2014**, *9*, 1415–1438.
19. Ade, S.B.; Kolhatkar, D.G.; Deshpande, M.N. Synthesis, characterization and biological activity of a schiff base derived from isatin and 2–amino, 4–methyl phenol and its transition metal complexes. *Int. J. Pharma. Bio. Sci.* **2012**, *3*, 350–356.
20. Baenziger, N.C.; Struss, A.W. Crystal structure of 2-sulfanilamidopyrimidinesilver(I). *Inorg. Chem.* **1976**, *15*, 1807. [CrossRef]
21. Cook, D.S.; Turner, M.F. Crystal and molecular structure of silver sulphadiazine (N1-pyrimidin-2-ylsulphanilamide). *J. Chem. Soc. Perkin Trans.* **1975**, *2*, 1021. [CrossRef]
22. Baenziger, C.; Modak, S.L.; Fox, C.L., Jr. Diamminebis(2-sulfanilamidopyrimidinato)zinc(II), $[Zn(C_{10}H_9N_4O_2S)_2(NH_3)_2]$. *Acta Crystallogr.* **1983**, *39*, 1620. [CrossRef]
23. Brown, C.J.; Cook, D.S.; Sengier, L. Bis[N^1-(2-pyrimidinyl)sulphanilamido]zinc–ammonia (1/2), $[Zn(C_{10}H_9N_4O_2S)_2].{}_2NH_3$. *Acta Crystallogr.* **1985**, *41*, 718. [CrossRef]
24. Weder, J.E.; Dillon, C.T.; Hambley, T.W. Copper complexes of nonsteroidal anti-inflammatory drugs: An Opportunity yet to be realized. *Coord. Chem. Rev.* **2002**, *232*, 95–126. [CrossRef]
25. Thompson, K.H.; McNeill, J.H.; Orvig, C. Vanadium Compounds as Insulin Mimics. *Chem. Rev.* **1999**, *99*, 2561. [CrossRef]
26. Shechter, Y.; Shisheva, A.; Gefel, D. *Chemistry, Biochemistry, and Therapeutic Applications*; Tracey, A.S., Crans, D.C., Eds.; Oxford University Press: New York, NY, USA, 1998; Volume 20.
27. Campos, M.M.A.; Gris, L.R.S. New gold(I) and silver(I) complexes of sulfamethoxazole: Synthesis, X-ray structural characterization and microbiological activities of triphenylphosphine(sulfamethoxazolato-N_2) gold(I) and (sulfamethoxazolato)silver(I) Inorg. *Chem. Commun.* **2007**, *10*, 1083–1087.

28. Garg, S.K.; Ghosh, S.S.; Mathur, V.S. Comparative pharmacokinetic study of four different sulfonamides in combination with trimethoprim in human volunteers. *Int. J. Clin. Pharm. Therapy. Toxicol.* **1986**, *24*, 23.
29. Holm, R.H.; Connor, M.J.O. The Stereochemistry of Bis-Chelate Metal(II) Complexes. *Prog. Inorg. Chem.* **1971**, *14*, 263.
30. Melagraki, G.; Afantitis, A.; Sarimveis, H.; Igglessi-Markopoulou, O.; Supuran, C.T. QSAR study on *para*-substituted aromatic sulfonamides as carbonic anhydrase II inhibitors using topological information indices. *Med. Chem.* **2006**, *14*, 1108–1114. [CrossRef]
31. Adamu, U.A.; Magaji, B.; Mohammad, A.B.; Sani, M.M.; Adoram, N. Synthesis, Characterization and Antibacterial Study of Co (II) and Cu (II) Complexes of Sulfamethoxazole. *AJARR* **2020**, *10*, 38–43. [CrossRef]
32. Mallikarjuna, N.M.; Keshavayya, J.; Maliyappa, M.R.; Shoukat Ali, R.A.; Venkatesh, T. Synthesis, characterization, thermal and biological evaluation of Cu (II), Co (II) and Ni (II) complexes of azo dye ligand containing sulfamethaxazole moiety. *J. Mol. Struct.* **2018**, *1165*, 28–36. [CrossRef]
33. Machado, A.P.; Anza, M.; Fischman, O. Bacillus subtilis induces morphological changes in Fonsecaea pedrosoi in vitro resulting in more resistant fungal forms in vivo. *J. Venom. Anim. Toxins Incl. Trop. Dis.* **2010**, *16*, 592–598. [CrossRef]
34. Molina-Hernandez, J.B.; Aceto, A.; Bucciarelli, T.; Paludi, D.; Valbonetti, L.; Zilli, K.; Scotti, L.; Chaves-López, C. The membrane depolarization and increase intracellular calcium level produced by silver nanoclusters are responsible for bacterial death. *Sci. Rep.* **2021**, *11*, 21557. [CrossRef]
35. Gasbarri, C.; Ronci, M.; Aceto, A.; Vasani, R.; Iezzi, G.; Florio, T.; Barbieri, F.; Angelini, G.; Scotti, L. Structure and Properties of Electrochemically Synthesized Silver Nanoparticles in Aqueous Solution by High-Resolution Techniques. *Molecules* **2021**, *26*, 5155. [CrossRef]
36. Tweedy, B.G. Synthesis, Characterization and Antibacterial Activity of Mixed Ligand (HL) Complexes Mn(ll), Co(ll), Ni(ll), Zn(ll), Cd(ll) and Hg(ll) with Azide (N3-). *Open J. Inorg. Chem.* **1964**, *55*, 910–918.
37. Kesimli, B.; Topacli, A. Infrared studies on Co and Cd complexes of Sulfamethoxazole. *Spectrochim. Acta Part A* **2001**, *57*, 1031–1036. [CrossRef]
38. El-Shwiniy, W.H.; Shehab, W.S.; Mohamed, S.F.; Ibrahium, H.G. Synthesis and cytotoxic evaluation of some substituted pyrazole zirconium (IV) complexes and their biological assay. *Appl. Organometal. Chem.* **2018**, *32*, 4503. [CrossRef]
39. Chavda, B.R.; Socha, B.N.; Pandya, S.B.; Chaudhary, K.P.; Padariya, T.J.; Alalawy, M.D.; Patel, M.K.; Dubey, R.P.; Patel, U.H. Coordination behavior of dinuclear silver complex of sulfamethoxazole with solvent molecule having static rotational disorder: Spectroscopic characterization, crystal structure, Hirshfeld surface and antimicrobial activity. *J. Mol. Struct.* **2021**, *1228*, 129777. [CrossRef]
40. Torre, M.; Calvo, S.; Pardo, H.; Mombru, A.W. Synthesis, spectroscopic characterization and crystal structure of disulfamethoxazole diaquo Ni(II) monohydrate. *J. Coord. Chem.* **2005**, *58*, 513–520. [CrossRef]
41. Venkatachalam, G.; Maheswaran, S.; Ramesh, R. Synthesis, Spectra, Redox property and catalytic activity of ruthenium Schiff base complexes. *Indian J. Chem.* **2005**, *44*, 705.
42. Lever, A.B.P. Electronic spectra of d^n ions. In *Inorganic Electronic Spectroscopy*, 2nd ed.; Elsevier: Amsterdam, The Netherlands, 1984.
43. El-Shwiniy, W.H.; Abbass, L.M.; Sadeek, S.A.; Zordok, W.A. Synthesis, Structure, DFT, and Biological Activity of Metal Complexes of Norfloxacin and Metformin Mixed Ligand. *Russ. J. Gen. Chem.* **2020**, *90*, 483. [CrossRef]
44. El-Shwiniy, W.H.; Gamil, M.A.; Sadeek, S.A.; Zordok, W.A.; El-farargy, A.F. Ligational, density functional theory, and biological studies on some new Schiff base 2-(2-hydroxyphenylimine) benzoic acid (L) metal complexes. *Appl. Organometal. Chem.* **2020**, *34*, 5696.
45. Sadeek, S.A.; Abd El-Hamid, S.M.; El-Shwiniy, W.H. Synthesis, spectroscopic characterization, thermal stability and biological studies of mixed ligand complexes of gemifloxacin drug and 2,2′-bipyridine with some transition metals. *Res. Chem. Intermed.* **2016**, *42*, 3183. [CrossRef]
46. Dhanaraj, C.J.; Nair, M.S. Synthesis, characterization, and antimicrobial studies of some Schiff-base metal(II) complexes. *J. Coord. Chem.* **2009**, *62*, 4018. [CrossRef]
47. Mohamed, G.G.; Sharaby, C.M. Metal complexes of Schiff base derived from sulphametrole and o-vanilin: Synthesis, spectral, thermal characterization and biological activity. *Spectrochim. Acta A* **2007**, *66*, 949–958. [CrossRef]